

Real-space observation of current-driven domain wall motion in submicron magnetic wires

A. Yamaguchi, T. Ono, and S. Nasu

Graduate School of Engineering Science, Osaka University, Toyonaka 560-8531, Japan

K. Miyake

Institute for Chemical Research, Kyoto University, Uji 611-0011, Japan

K. Mibu

Research Center for Low Temperature and Materials Sciences, Kyoto University, Uji 611-0011, Japan

T. Shinjo

International Institute for Advanced Studies, Soraku-gun, 619-0225, Japan

(Dated: October 23, 2018)

We report direct observation of current-driven magnetic domain wall (DW) displacement by using a well-defined single DW in a micro-fabricated magnetic wire with submicron width. Magnetic force microscopy visualizes that a single DW introduced in a wire is displaced back and forth by positive and negative pulsed-current, respectively. The direct observation gives quantitative information on the DW displacement as a function of the intensity and the duration of the pulsed-current. The result is discussed in terms of the spin-transfer mechanism.

In general, ferromagnets are composed of magnetic domains, within each of which magnetic moments align. The directions of magnetization of neighboring domains are not parallel. As a result, there is a magnetic DW between neighboring domains. The direction of moments gradually changes in a DW. What will happen if an electric current flows through a DW? Since the spin direction of conduction electrons changes when the electrons cross the DW, spin transfer from electrons into the DW occurs and torque is exerted on the DW. In consequence, the electric current can displace the DW[1, 2, 3, 4]. This current-driven DW motion has been confirmed by experiments on magnetic thin films and magnetic wires[5, 6, 7, 8, 9, 10]. However, quantitative experiment on a single DW in a magnetic wire for getting deeper insights into the physical mechanisms of this effect is still lacking. Our real-space observation by MFM gives the quantitative information: DW displacement as a function of the intensity and the duration of the pulsed-current. It is found that the DW displacement is proportional to the pulse duration and the DW velocity increases with the current density.

FIG. 1: Schematic illustration of a top view of the sample. One end of the L-shaped wire is connected to a diamond-shaped pad which acts as a domain wall (DW) injector, and the other end is sharply pointed to prevent a nucleation of a DW from this end. The wire has four electrodes made of Cu. MFM observations were performed for the hatched area at room temperature.

We designed a special L-shaped magnetic wire with a round corner as schematically illustrated in Fig. 1. One end of the L-shaped magnetic wire is connected to

FIG. 2: (a) MFM image after the introduction of a DW. DW is imaged as a bright contrast, which corresponds to the stray field from positive magnetic charge. (b) Schematic illustration of a magnetic domain structure inferred from the MFM image. DW has a head-to-head structure. (c) Result of micromagnetics simulation (vortex DW). (d) Result of micromagnetics simulation (transverse DW). (e) MFM image calculated from the magnetic structure shown in Fig. 2(c). (f) MFM image calculated from the magnetic structure shown in Fig. 2(d). (g) Magnified MFM image of a DW. (h) MFM image after an application of a pulsed-current from left to right. The current density and pulse duration are 1.2×10^{12} A/m² and 5 μ s, respectively. DW is displaced from right to left by the pulsed-current. (i) MFM image after an application of a pulsed-current from right to left. The current density and pulse duration are 1.2×10^{12} A/m² and 5 μ s, respectively. DW is displaced from left to right by the pulsed-current.

FIG. 3: (a)-(k) Successive MFM images with one pulse applied between each consecutive image. The current density and the pulse duration were 1.2×10^{12} A/m² and 0.5 μ s, respectively. Note that a tail-to-tail DW is introduced, which is imaged as a dark contrast.

a diamond-shaped pad which acts as a DW injector[11], and the other end is sharply pointed to prevent a nucleation of a DW from this end[12]. L-shaped magnetic wires of 10 nm-thick Ni₈₁Fe₁₉ were fabricated onto thermally oxidized Si substrates by means of an e-beam lithography and a lift-off method. The width of the wire is 240 nm. The wire has four electrodes made of nonmagnetic material, 20 nm-thick Cu, for electrical transport measurements. MFM observations were performed for the hatched area in Fig. 1 at room temperature. CoPtCr

low moment probes were used in order to minimize the influence of the stray field from the probe on the DW in the wire.

Because of the special shape of the wire, a single DW can be introduced from the diamond-shaped pad and it stops in the vicinity of the round corner when a magnetic field is applied along the wire axis connected to the pad[11, 13]. In order to introduce a DW at the position a little bit away from the corner, the direction of the external magnetic field was set 26 degrees from the wire axis in the substrate plane as shown in Fig.1. In the initial stage, a magnetic field of +1 kOe was applied in order to align the magnetization in one direction along the wire. Then, a single DW was introduced by applying a magnetic field of -175 Oe. After that, the MFM observations were carried out in the absence of a magnetic field. The existence of the single DW in the vicinity of the corner was confirmed as shown in Fig. 2(a). The DW is imaged as a bright contrast, which corresponds to the stray field from positive magnetic charge. In this case, a head-to-head DW is realized as schematically illustrated in Fig. 2(b). The position and the shape of the DW were unchanged after several MFM scans, indicating that the DW was pinned by a local structural defect as reported by Nakatani *et al.*[14] and that a stray field from the probe was too small to change the magnetic structure and position of the DW.

To clarify the magnetic structure of the head-to-head DW, micromagnetics simulations were performed by using micromagnetics simulator (OOMMF) from NIST[15]. The parameters used for the calculation were a unit cell size of 5 nm \times 5 nm with a constant thickness of 10 nm, a magnetization of 1.08 T, and a damping constant of $\alpha = 0.1$. The size of the calculated model was the same as the sample for the experiment except for the length of the wire. Two types of DWs, vortex and transverse DW, were obtained as a stable state in the absence of a magnetic field by changing the initial magnetization configuration. Figures 2(c) and 2(d) show the results of the micromagnetics simulations for the vortex and the transverse DW, respectively. Figures 2(e) and 2(f) show the MFM images calculated from the magnetic structures[16] shown in Figs. 2(c) and 2(d), respectively. By comparing the calculated MFM images with the observed high-resolution MFM image of the DW (Fig. 2(g)), it is concluded that the DW is the vortex type.

After the observation of Fig. 2(a), a pulsed-current was applied through the wire in the absence of a magnetic field. The current density and the pulse duration were 1.2×10^{12} A/m² and 5 μ s, respectively, and the rise and fall times were shorter than 15 ns. Figure 2(h) shows the MFM image after an application of the pulsed-current from left to right. The DW, which had been in the vicinity of the corner (Fig. 2(a)), was displaced from right to left by the application of the pulsed-current. Thus, the direction of the DW motion is opposite to the current

direction. Furthermore, the direction of the DW motion can be reversed by switching the current polarity as shown in Fig. 2(i). These results are consistent with the spin transfer mechanism[1, 2, 3, 4]. The critical current density j_c below which the DW cannot be driven by the current was observed to be about 1.0×10^{12} A/m².

Figures 3(a)-3(k) are successive MFM images with one pulsed-current applied between each consecutive image. The current density and the pulse duration were 1.2×10^{12} A/m² and 0.5 μ s, respectively. Prior to the MFM observation, a magnetic field of -1 kOe was applied in order to align the magnetization in the direction opposite to that in the previous experiment. Then, a tail-to-tail DW was introduced by applying a magnetic field of +175 Oe. The introduced DW is imaged as a dark contrast in Fig. 3, which indicates that a tail-to-tail DW is formed as schematically illustrated in Fig. 3. The direction of the tail-to-tail DW motion is also opposite to the current direction. The fact that both head-to-head and tail-to-tail DWs are displaced opposite to the current direction clearly indicates that the DW motion is not caused by a magnetic field generated by the current (Oersted field). Each pulse displaced the DW opposite to the current direction. The difference in the displacement for each pulse is possibly due to the pinning by randomly located defects. The average displacement per one pulse did not depend on the polarity of the pulsed-current.

We discuss the interpretation of the observed current-driven DW motion. The Joule heating by the pulsed-current should have some effect on the DW motion because it activates the thermal process. However, the heating cannot explain the fact that the direction of the DW motion is reversed by switching the current polarity. The effect of the Oersted field is also ruled out as mentioned above. Hydromagnetic DW-drag force associated with the Hall effect is negligible in films thinner than 0.1 μ m[17]. Therefore, only the spin transfer mechanism[1, 2, 3, 4] can explain our experimental results.

For more quantitative discussion, we investigated the DW displacement as a function of the duration and the intensity of the pulsed-current. Figure 4(a) shows the average DW displacement per one pulse as a function of the pulse duration under a condition of constant current density of 1.2×10^{12} A/m². The average DW displacement is almost proportional to the pulse duration, which indicates that the DW has a constant velocity of 3.0 m/s and the acceleration of the DW can be neglected in the time domain investigated. Figure 4(b) shows the average DW velocity as a function of the current density. The average velocity could be determined only in a narrow range of the current density from 1.1×10^{12} A/m² to 1.3×10^{12} A/m². Below 1.1×10^{12} A/m², the displacement for each pulse was not reproducible. Above 1.3×10^{12} A/m², the samples were degraded by the Joule heating due to the high current density. Although the

DW velocity was measured only in the small current density range, it was well confirmed that the DW velocity increases with the current density, as expected from the spin transfer mechanism.

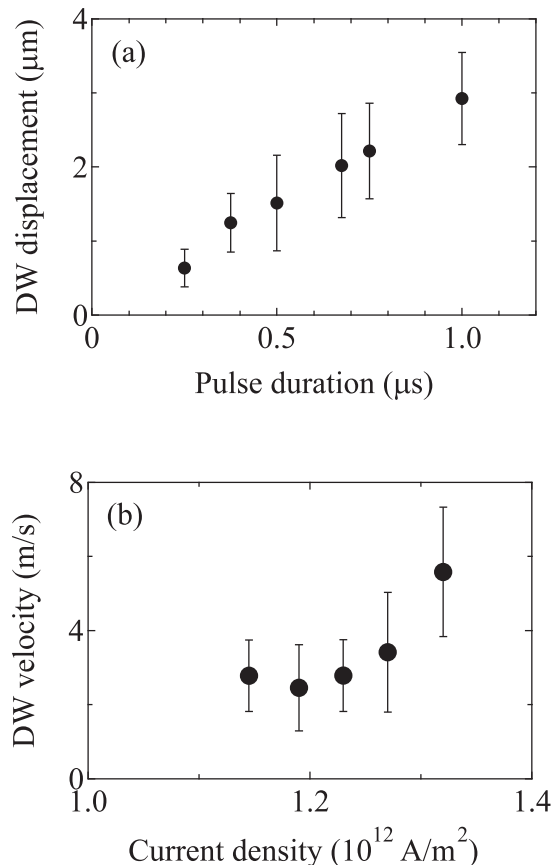


FIG. 4: (a) Average DW displacement per one pulse as a function of the pulse duration under a condition of constant current density of 1.2×10^{12} A/m². (b) Average DW velocity as a function of the current density.

Since the DW width in the present experiment is much larger than the Larmor precession length (several nm), the electron's spin can adiabatically follow the direction of the local magnetization[1, 2, 3, 4]. As a result, each electron passing through the DW flips its spin and gives a quantum \hbar of angular momentum to the DW. The displacement of the DW should be proportional to the amount of the transferred angular momentum, which is proportional to the duration of the pulsed-current. Thus, the finding that the DW displacement is proportional to the pulse duration supports that the observed DW motion is due to the spin-transfer. Here, we discuss the efficiency of the current-driven DW motion in the present experiments. The spin transfer from an electron adds magnetic moment of $2\mu_B$ to the DW, where μ_B is the Bohr magneton. Thus, the expected change of magnetic moment in the wire by the pulsed-current, $m_{current}$, is

calculated as $m_{current} = 2p\mu_B j S \Delta t / e$, where p is the spin-polarization of the current, j is the current density, S is the cross-sectional area of the wire, Δt is the pulse duration, and e is the electronic charge. On the other hand, the change of magnetic moment in the wire by the displacement of the DW, Δm , is calculated as $\Delta m = 2M_S \Delta l S$, where Δl is the displacement of the DW. Thus, we define the efficiency as $\eta = \Delta m / m_{current}$. From the definition, the efficiency is zero below j_c because the DW does not move below j_c . This means the transferred spin angular momentum dissipates into the environment possibly through the excitation of local spin waves in the DW. The efficiency increases with the current density and $\eta = 0.1$ at $j = 1.3 \times 10^{12}$ A/m² if we assume $p = 0.7$ [18].

We have shown the current-driven DW motion for a single DW with a well-defined magnetic structure in a submicron magnetic wire, which certifies the spintronic device operation[19, 20] by this effect. All experimental results are qualitatively consistent with the spin transfer mechanism[1, 2, 3, 4]. It was found that merely several percent of the transferred angular momentum was used for the displacement of the DW. This is possibly due to the complicated magnetic structure in the vortex DW. Detailed experiments by changing the thickness and the width of the wire are needed to elucidate the origin of the low efficiency.

We would like to thank Y. Suzuki, S. Yuasa, H. Kohno, and G. Tatara for valuable discussions. The present work was partly supported by the Ministry of Education, Culture, Sports, Science and Technology of Japan (MEXT), through the Grants-in-Aid for COE Research (10CE2004 and 12CE2005) and MEXT Special Coordination Funds for Promoting Science and Technology (Nanospintronics Design and Realization, NDR).

-
- [1] L. Berger, J. Appl. Phys., **55**, 1954 (1984).
 - [2] L. Berger, J. Appl. Phys., **71**, 2721, (1992).
 - [3] G. Tatara and H. Kohno, cond-mat/0308464.
 - [4] X. Waintal and M. Viret, cond-mat/0301293.
 - [5] P.P. Freitas and L. Berger, J. Appl. Phys. **57**, 1266 (1988).
 - [6] C.-Y. Hung and L. Berger, J. Appl. Phys. **63**, 4276 (1988).
 - [7] L. Gan, S.H. Chung, K.H. Ashenbach, M. Dreyer, and R.D. Gomez, IEEE Tran. Magn. **36** 3047 (2000).
 - [8] H. Koo, C. Krafft, and R.D. Gomez, Appl. Phys. Lett., **81**, 862 (2002).
 - [9] J. Grollier *et al.*, Appl. Phys. Lett., **83**, 509 (2003).
 - [10] N. Vernier *et al.*, cond-mat/0304549.
 - [11] K. Shigeto, T. Shinjo, and T. Ono, Appl. Phys. Lett. **75**, 2815 (1999).
 - [12] T. Schrefl, J. Fidler, K.J. Kirk, and J.N. Chapman, J. Magn. Magn. Mater. **175**, 193 (1997).
 - [13] D.A. Allwood *et al.*, Appl. Phys. Lett. **81**, 4005 (2002).

- [14] Y. Nakatani, A. Thiaville, and J. Miltat, *Nature Materials* **2**, 521 (2003).
- [15] <http://math.nist.gov/oommf/>.
- [16] H. Saito, J. Chen, and S. Ishio, *J. Magn. Magn. Mater.* **191**, 153 (1999).
- [17] L. Berger, *J. Appl. Phys.* **49**, 2156 (1978).
- [18] J. Bass and W.P. Pratt Jr., *J. Magn. Magn. Mater.* **200**, 274 (1999).
- [19] J.J. Versluijs, M.A. Bari, and J.M.D. Coey, *Phys. Rev. Lett.* **87**, 026601 (2001).
- [20] D.A. Allwood *et al.*, *Science*, **296**, 2003 (2002).

This figure "fig1.gif" is available in "gif" format from:

<http://arxiv.org/ps/cond-mat/0309124v2>

This figure "fig2.gif" is available in "gif" format from:

<http://arxiv.org/ps/cond-mat/0309124v2>

This figure "fig3.gif" is available in "gif" format from:

<http://arxiv.org/ps/cond-mat/0309124v2>